Available online at www.sciencedirect.com
ScienceDirect
Composites Science and Technology 67 (2007) 1139–1147
COMPOSITES SCIENCE AND TECHNOLOGY
www.elsevier.com/locate/compscitech

Mechanical properties and bioactivity of porous PLGA/TiO_2 nanoparticle-filled composites for tissue engineering scaffolds

F.G. Torres [a], S.N. Nazhat [b], S.H. Sheikh Md Fadzullah [c], V. Maquet [d], A.R. Boccaccini [c,*]

[a] *Polymers and Composites Group, Catholic University of Peru, Lima 32, Peru*
[b] *Division of Biomaterials and Tissue Engineering, UCL Eastman Dental Institute, 256 Gray's Inn Road, London WC1X 8LD, UK*
[c] *Department of Materials and Composites Centre, Imperial College London, Prince Consort Road, London SW7 2BP, UK*
[d] *University of Liège, Centre for Education and Research on Macromolecules, Sart-Tilman, B6, B-4000 Liège, Belgium*

Received 20 March 2006; received in revised form 17 May 2006; accepted 21 May 2006
Available online 13 July 2006

Abstract

Poly(lactide-co-glycolide) (PLGA) foams and PLGA/titanium dioxide (TiO_2) nanoparticle-filled composite foams (porosity > 90%) were produced by thermally induced solid–liquid phase separation (TIPS) and subsequent solvent sublimation. The scaffolds exhibit bimodal and anisotropic pore structures, with tubular macropores (approximately 100 μm in diameter) interconnected by a network of micropores. Quasi-static compression testing and dynamic mechanical analysis were carried out and the results were correlated to the microstructure observed by SEM, confirming the strong anisotropic behaviour of the foams. A study of the collapse mechanism of the foams porous structure revealed that when compressed in the main pore direction, the scaffolds failure mechanism involves an initial "accommodation" of large regions of the porous structure, followed by the collapse of individual pores in different modes. The bioactivity of the scaffolds was demonstrated by immersion in simulated body fluid (SBF) for up to 28 days. Formation of hydroxyapatite crystals on the scaffold surface was confirmed by X-ray diffraction analysis.

Keywords: A. Particle reinforced composite; B. Mechanical properties; B. Porosity; C. Anisotropy; Tissue engineering scaffolds

1. Introduction

Tissue engineering offers an alternative approach to the repair and regeneration of damaged human tissue. The principle involved is the regeneration of living tissue, where loss or damage has occurred as a result of injury or disease [1,2]. The scientific challenge encompasses understanding the cells themselves, their mass transport requirements and biological environment, in conjunction with the development of optimal scaffold materials, which are usually porous and biodegradable, and act as temporary three-dimensional (3D) templates for cell adhesion, growth and proliferation [3]. Synthetic biodegradable polymer matrix composites incorporating bioactive ceramic phases are being increasingly considered for use as tissue engineering scaffolds due to their improved physical, biological and mechanical properties, as well as having the capacity for tailoring their structure and degradation rate to the specific need at the implant site [4–6]. In general, scaffolds should have appropriate mechanical properties, e.g. elastic constants, with values in a similar range to those of the tissues at the site of implantation. Much research is focused on the development of such porous bioactive and biodegradable composite scaffolds for the repair and regeneration of bone tissue [6–10]. Among this group of materials, porous degradable polyglycolide, polylactide, or their co-polymers, are especially relevant for bone tissue engineering, with additions of inorganic particles or fibres, such as bioactive glass and hydroxyapatite (HA) to impart bioactivity and improve mechanical properties [11–15]. Processing of materials using the thermally induced phase separation

* Corresponding author.
E-mail address: a.boccaccini@imperial.ac.uk (A.R. Boccaccini).

0266-3538/$ - see front matter © 2006 Elsevier Ltd. All rights reserved.
doi:10.1016/j.compscitech.2006.05.018

(TIPS) method enables the production of highly porous foams which exhibit pore anisotropy and high pore interconnectivity, which may be controlled to enable the fabrication of scaffolds with tailored porosity, appropriate to the tissue in concern [7,16].

TiO_2 nanoparticles have been recently proposed as attractive filler materials for biodegradable polymer matrices since they enhance cell attachment and proliferation on the composite surfaces [17]. Most previous research on polymer/TiO_2 nanoparticle composites has been carried out, however, on dense 2D surfaces (films), and there is virtually no previous work focusing on the incorporation of TiO_2 nanoparticles as filler in 3D porous scaffolds.

In the present investigation poly(D,L-lactide-co-glycolide) (PLGA)/TiO_2 nanoparticle foams have been fabricated for the first time by TIPS. The focus of the study is on the characterisation of the foams pore structure and on the measurement and analysis of their mechanical properties.

2. Experimental

2.1. Materials

Poly (D,L-lactide-co-glycolide) (PLGA) co-polymer with a 75:25 LA:GA molar ratio and low molecular weight with an inherent viscosity of 0.61 dl/g was provided by Alkermes (Cincinnati, Ohio, USA). The manufacturer indicates that the polymer is completely amorphous with a specific gravity and Young's modulus of 1.2 g cm^{-3} and 1.37 GPa, respectively. Dimethylcarbonate (DMC, of >99% purity) was purchased from Sigma–Aldrich and used as solvent.

Commercially available TiO_2 nanopowder (Aeroxide® P25, Degussa, Frankfurt a. M., Germany) with a mean primary size of 21 nm, specific surface area of 50 m^2 g^{-1} and density 3.966 g cm^{-3} was used. The crystalline structure of the nanoparticles consist of approximately 70% anatase and 30% rutile.

2.2. Foam fabrication

PLGA and PLGA/TiO_2-filled composite foams were prepared by thermally induced phase separation (TIPS) and subsequent solvent sublimation, which has been described in detail elsewhere [7,14,16]. Briefly, PLGA was dissolved in DMC at a polymer weight to solvent volume ratio of 5% (w/v). The mixture was stirred overnight to obtain a homogeneous polymer solution. Given quantities of TiO_2 particles were added to the polymer solution, which was then transferred to a lyophilisation flask and sonicated for 15 min to achieve a homogeneous distribution of TiO_2 particles in the solution and to break up agglomerates. The flask was then immersed in liquid nitrogen and maintained at −196 °C for 2 h. The frozen mixture was placed under vacuum (10^{-2} Torr) and transferred to an ethylene glycol bath, which was maintained at −10 °C. The solvent was sublimed at −10 °C for 48 h and then at 0 °C for a further 48 h. Finally, the resulting foam monolith (of 90 mm diameter and 10 mm thickness) was completely dried at room temperature in a vacuum oven until reaching constant weight. The following foam systems were investigated: neat PLGA and composite foams filled with TiO_2particles at 5 wt% and 20 wt%.

2.3. Characterisation techniques

2.3.1. Morphological Characterisations through SEM

Surface morphology, microstructure homogeneity as well as uniformity of TiO_2 particle distribution in the composites were characterised using scanning electron microscopy (SEM) (JEOL JSM). Specimens were mounted onto stubs using adhesive tapes and sputtered with a gold layer. Accelerating voltages in the range of 6–18 kV were used for the observation of cross-sections and surface topography.

2.3.2. Overall apparent density

The volume and mass of cubic foam specimens (approximately $5 \times 5 \times 5$ mm^3) were determined. Measurements of the overall dimensions were taken using vernier callipers (across 20 samples per composition). Using the densities of TiO_2 (3.96 g cm^{-3}) and PLGA (1.2 g cm^{-3}) a theoretical porosity was calculated based on the volume percentage of TiO_2 in the foam and by comparing its apparent density to the bulk system according to Eq. (1):

$$P = 1 - \frac{\rho}{\rho_0} \tag{1}$$

where ρ is the foam density and ρ_0 is the density of the non-porous material.

2.3.3. Mechanical analysis

Quasi-static compression tests were carried out using the static stress scan mode of analysis of a Pyris run DMA7e (Perkin–Elmer Instruments). Specimens were cut from the most homogeneous region [18] of the foam to form cubes measuring $5 \times 5 \times 5$ mm^3. Compressive mechanical tests were conducted in the axial (parallel to the tubular pores) and transverse (perpendicular to the tubular pores) directions using the parallel plate set up. Specimens were tested under compression from 2 kPa to 300 kPa at a rate of 20 kPa min^{-1}. The stress and modulus response to strain were recorded. The axial modulus, the yield stress (defined as the end of the linear deformation region) and the corresponding strain at yield point were also recorded.

Dynamic mechanical analysis (DMA) was also carried out on cubic samples obtained from the homogeneous region of each of the three foam systems. Five repeat specimens were tested in compression under the stress control mode, where a static stress of 30 kPa was initially applied followed by a dynamic stress of 24 kPa. A temperature scan from 22 to 65 °C at a heating rate of 4 °C min^{-1} was applied. Nitrogen was used as purge. The viscoelastic parameters of storage modulus (E'), and mechanical loss tangent ($\tan\delta$) were recorded as a function of temperature.

The PLGA glass transition temperature (T_g) was taken as the peak obtained in $\tan\delta$.

2.3.4. Immersion in simulated body fluid (SBF)

In vitro bioactivity studies were carried out using simulated acellular body fluid (SBF) based on the formulation and method developed by Kokubo et al [19]. Briefly, the SBF, which has inorganic ion concentrations similar to those of human extracellular fluid, was prepared by dissolving respective amounts of reagent chemicals (all purchased from Sigma, Steinheim, Germany) of NaCl, $NaHCO_3$, KCl, $K_2HPO_4 \cdot 3H_2O$, $MgCl_2 \cdot 6H_2O$, $CaCl_2 \cdot 2H_2O$, and Na_2SO_4 into distilled water. The SBF was adjusted to physiological pH (pH 7.25) by HCl and buffered by tris(hydroxyl-methyl) aminomethane. After solvent evaporation overnight, the specimens attached to the cover glass were placed in 24-well plates using tweezers, and subsequently an aliquot (2 mL) of SBF (37 °C) was added to the specimens. During the immersion period, the specimens were kept at 37 °C in a humidified incubator, and the SBF was refreshed after 6 h of incubation followed by 24, 48 h and then after every three days. The specimens were then collected after 1, 3, 7, 14 and 28 days of incubation. The samples were rinsed in distilled water three times, then vacuum dried for 3 h and finally stored in desiccators for further examination. Powder X-ray diffraction (XRD) was performed using a Philips PW 1710 diffractometer in order to characterise the crystalline phases in the specimens and the possibly formed hydroxyapatite crystals after immersion in SBF. The specimens were exposed to high energetic (CuKα, $\lambda = 1.5406$ Å) X-rays and the 2θ angles were recorded using a scintillation counter in the 2θ interval between 5° and 75° at scan steps sizes of 0.04° and a detection time of 1.5 s per scan.

Mechanical analysis under compression stresses, as detailed above (Section 2.3.3) were also carried out on samples that had been treated in SBF for 28 days.

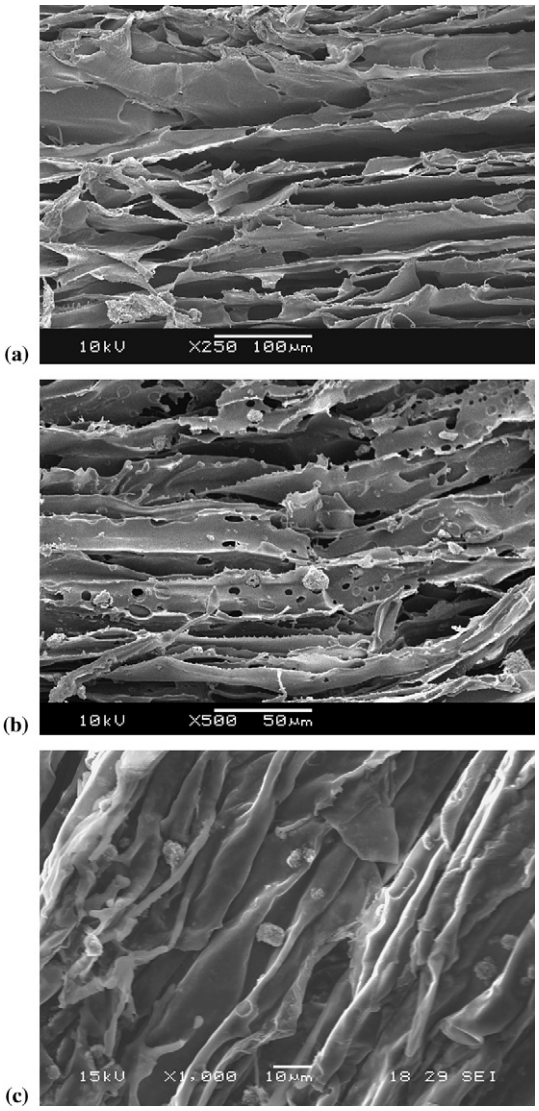

Fig. 1. SEM images of foam scaffolds in axial direction: (a) plain PLGA, (b) PLGA + 5 wt% TiO_2 and (c) PLGA + 20 wt% TiO_2. Some TiO_2 agglomerates are seen in the 20 wt% foam.

3. Results and discussion

3.1. Microstructural characterisation

By manipulating the parameters of the TIPS process (i.e., polymer to solvent ratio) the porous architecture can be controlled, and the presence of orientated tubular macropores can be determined [20], as observed in Fig. 1(a)–(c). In some cases both anisotropic pore architecture and mechanical properties may be beneficial for applications where the structure needs to have regions of crush resistance, for example in scaffolds of tubular shape [21]. From Fig. 1(b) it can be observed that PLGA + 5 wt% TiO_2 foams exhibit the presence of micropores in the cell walls. This is an undesired effect most probably due to the fact that the optimal processing conditions were not attained during the TIPS process. Fig. 1(c) shows the microstructure of a PLGA scaffold with 20 wt% of TiO_2 nanoparticle addition. Some agglomerates of TiO_2 nanoparticles can be observed on the polymer surface. The overall apparent density and porosity data are summarised in Table 1. The apparent porosity for these foams was greater than 90% with the PLGA + 5 wt% TiO_2 showing the highest level at 94.2% while the PLGA + 20 wt% TiO_2 having the lowest porosity at 90.9%.

Table 1
Apparent density and porosity of PLGA and PLGA/TiO_2 nanoparticle foams

TiO_2 content (wt%)	TiO_2 content (vol%)	App. density (ρ) (g cm^{-3})	Calculated avg. porosity (%) (P from Eq. (1))
0	0	0.088 ± 0.006	92.6
5	1.48	0.066 ± 0.003	94.7
20.00	6.67	0.127 ± 0.014	90.9

3.2. Mechanical properties: testing

Compressive mechanical tests were conducted in the axial (parallel to the tubular pores) and transverse (perpendicular to the tubular pores) directions using cubic samples. Fig. 2 shows typical stress–strain behaviours for these composite foams tested in the axial direction. All compositions initially showed a proportional increase of stress with strain, which is in agreement with the behaviour of cellular solids discussed in the literature [22,23]. Two further regions followed; a plateau due to the plastic collapse and buckling of the cell elements, and a further region where the stress increases rapidly due to the effective densification of the foam structure.

Table 2 shows the mechanical properties of PLGA/TiO_2 foams tested in compression in the axial direction. From Table 2 it can be observed that PLGA + 5 wt% TiO_2 foams resulted in the lowest modulus and stress values of all foam types studied which confirms that the cell walls are actually less resistant for these materials. This may be associated to the presence of micropores in the cell walls in these composites and the corresponding low apparent density (Table 1). It can also be noted that samples with 20 wt% TiO_2 show an increase in the Young's modulus of almost twice that of the pure PLGA foams. This apparent increase in modulus may also be due to the lower porosity of the PLGA + 20 wt% TiO_2. For comparison, tests were also conducted with the load applied perpendicularly to the direction of the macropores (data not shown). This transverse mechanical behaviour in compression displayed a distinctly different response to that of the axial loading. There appeared to be no obvious microfailure response due to buckling of the tubular macropores. Indeed the behaviour of all foams seemed to be dominated by the effect of massive densification of the foams. Testing in both directions has confirmed thus the mechanical anisotropy of the foams produced, which is typical for porous materials produced by the TIPS process as discussed in a previous work [18].

Table 2
Compression properties of PLGA/TiO_2 samples in as-fabricated condition tested via quasi-static compression testing in axial direction (axial modulus calculated from the slope of the stress–strain curve)

Sample	Axial modulus (MPa)	Yield stress (kPa)	Strain at yield point (%)
Plain PLGA	0.96 ± 0.33	108.93 ± 51.54	10.50 ± 3.15
PLGA + 5 wt% TiO_2	0.63 ± 0.30	69.87 ± 20.45	8.47 ± 1.41
PLGA + 20 wt% TiO_2	1.54 ± 0.41	118.00 ± 7.55	8.14 ± 1.71

3.3. Mechanical properties: modelling

An attempt to predict the elastic constants of the foams was undertaken. The apparent density (ρ) of the scaffolds was determined by using the measured mass and volume of the foams (Table 1). Porosity (P) was calculated using Eq. (1). The Gibson and Ashby model [23] given by Eq. (2) has generally been applied to relate the modulus to the density of foams:

$$\frac{E}{E_0} = C\left(\frac{\rho}{\rho_0}\right)^n = C(1-P)^n \tag{2}$$

where E is the modulus of the foam, E_0 and ρ_0 are the modulus and density of the completely dense material, respectively. The constants C and n depend on the foam microstructure. The value of n generally lies in the range $1 < n < 4$ giving a wide range of values for E/E_0 at a given density [24]. It has been suggested that for closed-cell porous systems n should have a value in the range of $1 < n < 2$. However, the dependence of C and n on the microstructure

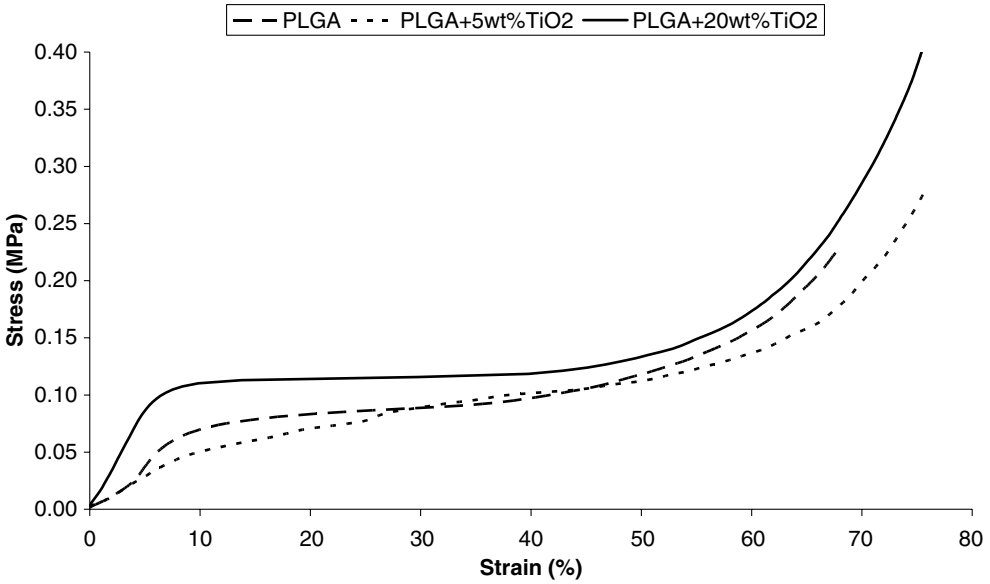

Fig. 2. Representative curve of plain PLGA foam showing axial compression stress and modulus in response to strain tested in longitudinal direction, e.g. parallel to the axis of tubular pores.

of highly porous materials with more complex pore structures such as the foams investigated here is not well understood [23]. Several important factors affect the stiffness–porosity relationship such as whether the pores are open or closed, their geometrical arrangement, in terms of pore orientation and shape, as well as the thickness of the pore walls, and whether the material is periodic or disordered. In their model, Roberts and Garboczi [24] found that if more than 70% of the cell faces are removed, n should increase to 2, indicating that edge bending becomes the dominant mechanism of deformation.

The effect of incorporating TiO_2 into the PLGA porous structure and the ability of Eq. (2) to predict the mechanical anisotropy of composite foams were assessed by calculating n values based on the experimental data, assuming a value $C = 1$, as done in our earlier study [18]. Our approach used the rule of mixtures (ROM), Ishai–Cohen [25], and Narkis models [26] to determine the effective modulus of non-porous composite systems with 5 and 20 wt% TiO_2 and applying the Gibson and Ashby model (Eq. (2)) using P values derived from the apparent density measurements (Table 1) to calculate n values. The elastic modulus of the composite E_c, as predicted by the Ishai–Cohen model [25] can be written as:

$$E_c = E_m\left(1 + \frac{v_f}{m/(m-1) - v_f^{1/3}}\right) \quad (3)$$

where v_f is the volume fraction of the reinforcement and m is the ratio of reinforcement to polymer modulus ($m = E_f/E_m$). The Narkis model [26] can be written as:

$$E_c = \frac{E_m}{K^*(1 - v_f^{1/3})} \quad (4)$$

where v_f is the volume fraction of the reinforcement and K^* is a stress concentration factor in the range 1.4–1.7. In this case, 1.4 has been used for K^*. This model is suitable for spherical inclusions at volume concentrations in the range 10–50%.

The modulus of TiO_2 is 230 GPa [27] and that of the PLGA matrix quoted by the manufacturer is 1.37 GPa. The modulus of the porous material is calculated by substituting E_c for E_0 into Eq. (2). The resultant n values are shown in Table 3. These n values are consistent with the data presented in the literature on the modulus of porous materials [23,24]. It is clear that the inclusion of TiO_2 particles has only a limited effect on the n value, as the calculated n values for samples with 0, 5 and 20 wt% TiO_2 are within 3–4% for the Ishai–Cohen and Narkis models. The rule of mixtures model shows an increase of around 30% in the value of n at 20 wt% of TiO_2 with regard to the other models used. This suggests that the rule of mixtures fails to predict the behaviour of this type of foams. Based on the previous observations, it is thus confirmed that the porous structure is not strongly affected by the incorporation of TiO_2, which is in agreement with previous work on similar TIPS produced composite foams as reported in the literature [7].

Table 3
Calculated n values in Eq. (2) that best fit experimental data, obtained using the rule of mixtures, Ishai–Cohen [25] and Narkis [26] models for the modulus of the composite materials

	Axial compression n values (ROM)	Axial compression n values (Ishai–Cohen)	Axial compression n values (Narkis)
Neat PLGA foam	2.86	2.86	2.72
PLGA/5 wt% TiO_2	2.97	2.54	2.51
PLGA/20 wt% TiO_2	3.99	2.98	3.01

3.4. Failure mechanisms

Controlled quasi-static compression tests were carried out to determine the collapse and failure mechanisms that occur during deformation of the PLGA based composite foams as investigated through SEM. Fig. 3(a) shows a panoramic view of a collapsed PLGA/TiO_2 (20 wt% TiO_2) composite specimen at a compression strain of 64%. Various macroregions with pores oriented in different directions can be observed. This is associated to a first collapse phase consisting in the accommodation of the pores forming well defined macroregions. Details from this and other SEM micrographs have shown that after initial accommodation of the macroregions takes place, individual cell collapse occurs according to their new accommodated orientations with regard to the direction of the applied load. Therefore, structures showing cell wall buckling (Fig. 3(b)) can be observed. A final stage of massive densification can also be observed in some of the structures at the higher final strains (Fig. 3(c)). Such densification results in increased final modulus of the composite (see Section 3.2). In connection with the deformation mechanisms and mechanical properties investigated, it should be emphasised that the structural integrity of the scaffolds is not sufficient for applications in load-bearing applications. This is however true also for most highly porous scaffold systems developed from combinations of polymers and inorganic fillers, as discussed elsewhere [28].

3.5. Dynamical mechanical analysis

Dynamic mechanical analysis (DMA) was carried out to investigate viscoelastic parameters of storage modulus (E') and $\tan\delta$ as a function of temperature and to locate the glass transition temperature of PLGA as obtained from the peak in $\tan\delta$. Fig. 4(a) and (b) shows representative storage modulus and $\tan\delta$ values of the various materials as a function of temperature, respectively. The storage modulus represents the elastic component of a material and is an indicator of the capability of a material to store energy during deformation. From the results, as illustrated in Fig. 4(a) and Table 4, it is observed that E' showed increased values

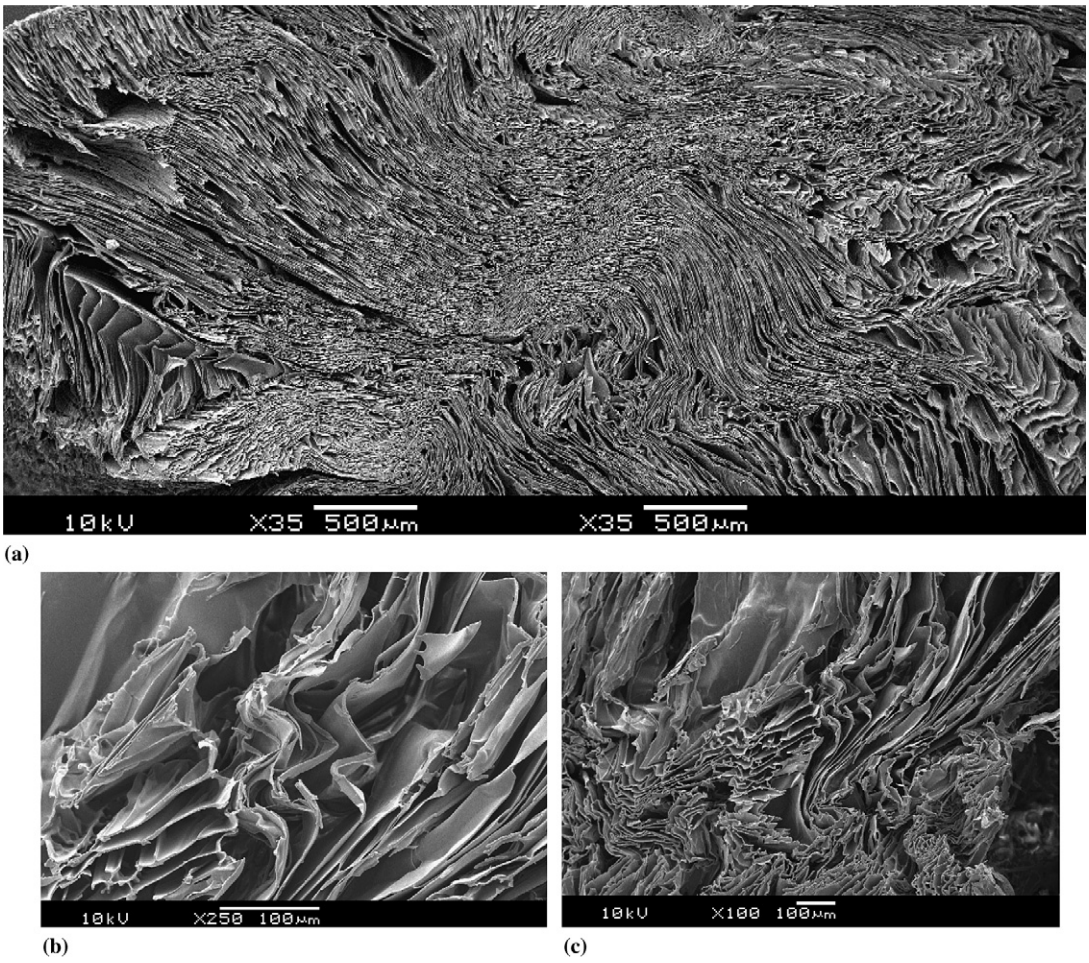

Fig. 3. (a) Panoramic SEM image of PLGA/TiO_2 (20 wt%) scaffold compressed in the longitudinal direction showing the "accommodated" pore regions after failure. (b) Detail of cell wall buckling of a PLGA/TiO_2 (20 wt%) foam showing the periodic nature of this type of failure. (c) Cell wall buckling and densification in a PLGA/TiO_2 (20 wt%) composite foam after compression loading.

for the PLGA + 20 wt% TiO_2 composites compared to the unreinforced PLGA. However, a decrease in storage modulus was observed for the composites containing 5 wt% TiO_2 nanoparticles, which was consistent with the results from the quasi-static compressive modulus values (Section 3.2). This is also related to the microporosity found in the struts of these samples (Fig. 1(b)). All composite foams showed an apparent increase in storage modulus as the temperature increased which was due to the apparent densification of the foams as the matrix approached the glass transition temperature [18,29]. Above PLGA-T_g, the storage modulus decreased with temperature.

To analyse the efficiency of reinforcement of the TiO_2 filler at 37 °C [30,31], relative modulus values were calculated according to Eq. (5) below:

$$E_r^I = \frac{E_c^I}{E_m^I} \tag{5}$$

where E_r^I is the relative storage modulus, E_c^I is the storage modulus of PLGA composite scaffolds with 5 and 20 wt% of TiO_2 addition and E_m^I is the storage modulus of plain PLGA. A decrease in modulus is observed for PLGA/5 wt% TiO_2 composite with regard to the plain polymer, while an increase in modulus is observed for composites with 20 wt% TiO_2 addition, although this increase in modulus was not statistically significant.

$\tan\delta$ is calculated from the ratio of loss to storage modulus and it is an indication of the energy lost due to damping. The results for $\tan\delta$ are given in Table 4. There was no significant change in $\tan\delta$ with addition of TiO_2. The matrix glass transition temperature on the other hand showed a reduction with addition of 20 wt% TiO_2 compared to the other foam compositions.

3.6. Immersion studies in simulated body fluid (SBF)

Immersion of samples in SBF is the method usually applied to assess bioactivity of materials, which is determined by the formation of hydroxyapatite on materials surfaces upon different periods of immersion in SBF [6,7,14]. In the present experiments, samples were examined after 28 days of immersion in SBF. SEM micrographs, as depicted for example in Fig. 5, indicated that there was a change in the structure and morphology of the foams after

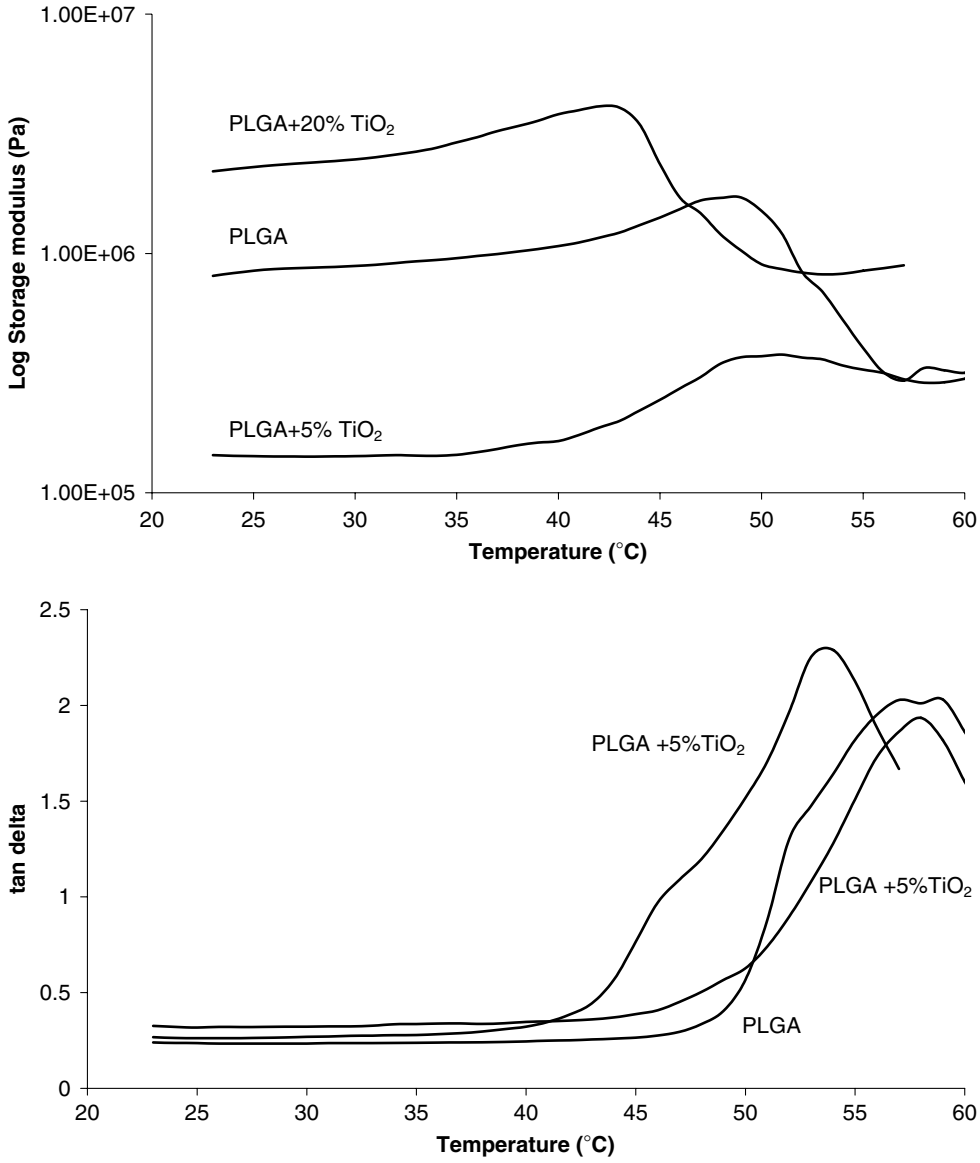

Fig. 4. Representative DMA curves for (a) storage modulus and (b) tan δ of PLGA and PLGA/TiO_2 foams.

Table 4
Viscoelastic parameters: storage modulus (E') and tan δ as a function of temperature for the different materials investigated, obtained by dynamical mechanical analysis

Material	E' (MPa) at Temperature (°C)			tan δ at Temperature (°C)			T_g
	23	37	45	23	37	45	
Plain PLGA	0.82 ± 0.37	0.97 ± 0.46	1.31 ± 0.6	0.26 ± 0.02	0.26 ± 0.02	0.29 ± 0.04	56.7 ± 1.1
PLGA + 5 wt% TiO_2	0.15 ± 0.01	0.17 ± 0.03	0.27 ± 0.04	0.38 ± 0.08	0.33 ± 0.01	0.38 ± 0.02	57.6 ± 0.4
PLGA + 20 wt% TiO_2	1.48 ± 0.91	2.18 ± 1.06	2.13 ± 0.30	0.30 ± 0.09	0.38 ± 0.09	0.78 ± 0.02	53.2 ± 0.9

Values of T_g are also shown.

28 days of immersion in SBF. The XRD patterns of neat PLGA and of PLGA/TiO_2 composites after immersion in SBF for 28 days are illustrated in Fig. 6. The scaffolds made with PLGA + 5 wt% TiO_2 show a sharp peak at approximately 32.8° angle which corresponds to the main crystalline hydroxyapatite peaks, indicating the possible formation of hydroxyapatite (HA) on the surfaces of the foam after exposure in SBF for 28 days. Similar results were found on foams containing 20 wt% TiO_2. The bioactive behaviour of the present composites is, as expected, similar to that of equivalent composites made with PDLLA matrix, as characterised elsewhere [32]. The possible effect of the presence of TiO_2 nanoparticles on the acidic degradation behaviour of the PLGA matrix remains to be inves-

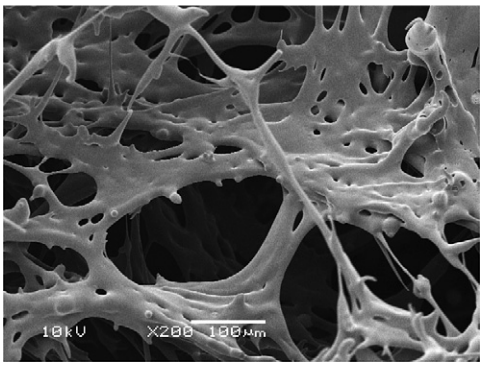

Fig. 5. SEM micrograph of a PLGA + 20 wt% TiO_2 foam after 28 days in SBF.

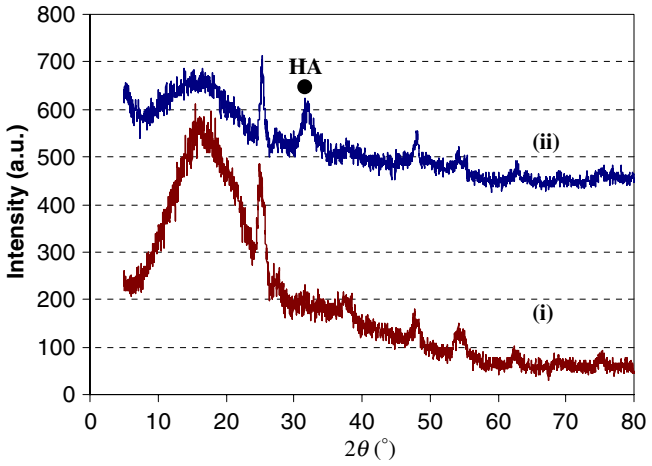

Fig. 6. XRD patterns of (i) plain PLGA and (ii) PLGA + 5 wt% TiO_2 after 28 days in SBF. HA is detected only in the composite foam.

tigated. As it is well known, there is a need to counterbalance the change of local pH upon degradation of PLGA (and PLA based polymers) as possible inflammatory reactions could occur in the surrounding tissue upon the degradation of the scaffold [15,21]. This buffering mechanisms is in fact one of the reasons behind the design of composite materials for tissue engineering [7].

As a preliminary assessment of the variation of mechanical properties of PLGA/TiO_2 composite scaffolds upon immersion in SBF, quasi-static compression strength tests were carried out on samples that had been immersed in SBF for 28 days. Prior to the test the samples were rinsed with deionised water and dried in vacuum. No significant differences in the modulus values were measured. A more detailed investigation should be carried out, however, to assess the time-dependant variation of the mechanical properties of the foams in SBF and to ascertain how the presence of TiO_2 nanoparticles affects the polymer degradation kinetics.

4. Conclusions

Composite foam scaffolds with >90% porosity were produced from PLGA and TiO_2 nanoparticles by means of the TIPS process. The scaffolds exhibit bimodal and anisotropic pore structure, with tubular macropores (approximately 100 μm in diameter) interconnected by a network of micropores. The anisotropic character of the mechanical behaviour of the foams was confirmed by quasi-static compression strength tests. Results for the composite moduli obtained from dynamic mechanical analysis confirmed the tendency observed with quasi-static compression tests. An increase in storage modulus was observed with addition of 20 wt% TiO_2, with regard to the unfilled PLGA. A study of the collapse mechanism of the porous structures revealed that when compressed in the main pore direction, the scaffolds failure behaviour involves the initial "accommodation" of large regions of the pore structure, followed by the collapse of individual pores in different modes. Certainly the structural integrity of the scaffolds is insufficient for load-bearing applications in bone tissue engineering. An analytical model based on the combination of available equations in the literature was proved to be successful for prediction of the modulus of the present foams. After 28 days of immersion in SBF, the composite scaffolds exhibit evidence of formation of hydroxyapatite on their surfaces, as detected by XRD. However the quantitative investigation of the possible in vitro bioactive character of these scaffolds as well as of the time-dependant variation of mechanical properties in SBF remains the scope for future research. Moreover the possible effect of the TiO_2 addition on the variation of local pH on degradation of the PLGA matrix has not been addressed. The PLGA foams developed here containing TiO_2 nanoparticles represent alternative systems to previously investigated PLGA/bioactive glass composites [7]. The two foam systems should be compared in their cellular in vitro and in vivo performance with the aim to choose the optimal system for bone tissue engineering applications.

Acknowledgements

SNN thanks the EPSRC UK for funding. CERM (Liege, Belgium) is indebted to the "Politique Scientifique Fédérale" in the frame of the "Pôles d'Attraction Interuniversitaires (5/03): Chimie et Catalyse Supramoléculaire", for financial support. FT thanks the Royal Society for a fellowship to visit Imperial College London.

References

[1] Langer R, Vacanti J. Tissue engineering. Science 1993;74:920–6.
[2] Hench LL, Polak JM. Third-generation biomedical materials. Science 2002;295:1014–7.
[3] Hutmacher DW. Polymeric scaffolds in tissue engineering bone and cartilage. Biomaterials 2000;21:2529–43.
[4] Devin JE, Attawia MA, Laurencin CT. Three-dimensional degradable porous polymer–ceramic matrices for use in bone repair. J Biomater Sci Polym Edn 1996;7:661–9.
[5] Taboas JM, Maddox RD, Krebsbach PH, Hollister SJ. Indirect solid free form fabrication of local and global porous, biomimetic and composite 3D polymer–ceramic scaffolds. Biomaterials 2003;24:181–94.

[6] Boccaccini AR, Roether JA, Hench LL, Maquet V, Jérôme R. A composites approach to tissue engineering. Ceram Eng Sci Proc 2002;23:805–15.
[7] Boccaccini AR, Maquet V. Bioresorbable and bioactive polymer/Bioglass® composites with tailored pore structure for tissue engineering applications. Comp Sci Technol 2003;63:2417–23.
[8] Thomson RC, Shung AK, Yaszemski MJ, Mikos AG. Polymer scaffold processing. In: Lanza RP, Langer R, Vacanti J, editors. Principles of tissue engineering. London: Academic Press; 2000.
[9] Laurencin CT, Lu HH. Polymer–ceramic composites for bone-tissue engineering. In: Davies JE, editor. Bone engineering. Toronto (Canada): Emsquared incorporated; 2000. p. 462–72.
[10] Wu L, Ding J. In vitro degradation of three-dimensional porous poly(D,L-lactide-co-glycolide) scaffolds for tissue engineering. Biomaterials 2004;25:5821–30.
[11] Zhang K, Ma Y, Francis LF. Porous polymer/bioactive glass composites for soft-to-hard tissue interfaces. J Biomed Mater Res 2002;61:551–63.
[12] Zhang K, Wang Y, Hillmyer MA, Francis LF. Processing and properties of porous poly(L-lactide)/bioactive glass composites. Biomaterials 2004;25:2489–500.
[13] Thomson RC, Yaszemski MJ, Powers JM, Mikos AG. Hydroxyapatite fiber reinforced poly(α-hydroxy ester) foams for bone regeneration. Biomaterials 1998;19:1935–43.
[14] Roether JA, Boccaccini AR, Hench LL, Maquet V, Gautier S, Jérôme R. Development and in-vitro characterisation of novel bioresorbable and bioactive composite materials based on polylactide foams and Bioglass® for tissue engineering applications. Biomaterials 2002;23:3871–8.
[15] Maquet V, Boccaccini AR, Pravata L, Notingher I, Jerome R. Porous poly(α-hydroxyacid)/Bioglass(R) composite scaffolds for bone tissue engineering. I: Preparation and in vitro characterisation. Biomaterials 2004;25:4185–94.
[16] Schugens C, Maquet V, Grandfils C, Jérôme R, Teyssié P. Biodegradable and macroporous polylactide implants for cell transplantation: 1. Preparation of macroporous polylactide supports by solid–liquid phase separation. Polymer 1996;37:1027–38.
[17] Savaiano JK, Webster TJ. Altered responses of chondrocytes to nanophase PLGA/nanophase titania composites. Biomaterials 2004;25:1205–13.
[18] Blaker JJ, Maquet V, Jerome R, Boccaccini AR, Nazhat SN. Mechanical properties of highly porous PDLLA/Bioglass® composite foams as scaffolds for bone tissue engineering. Acta Biomater 2005;1:643–52.
[19] Kokubo T, Kushitani H, Sakka S, Kitsugi T, Yamamuro T. Solutions able to reproduce in vivo surface-structure changes in bioactive glass-ceramic A-W. J Biomed Mater Res 1990;24:721–34.
[20] Maquet V, Blacher S, Pirard R, Pirard JP, Vyakarnam MN, Jérôme R. Preparation of macroporous biodegradable poly(L-lactide-co-epsilon-caprolactone) foams and characterisation by mercury intrusion porosimetry, image analysis, and impedancy spectroscopy. J Biomed Mater Res 2003;66A:199–213.
[21] Blaker JJ, Day RM, Maquet V, Boccaccini AR. Novel Bioresorbable poly(lactide-co-glycolide) (PLGA) and PLGA/Bioglass® composite tubular foam scaffolds for tissue engineering applications. Mater Sci Forum 2004;455–456:415–9.
[22] Hilyard NC. Mechanics of cellular plastics. London: Applied Science Publishers; 1982. p. 73–87.
[23] Gibson LJ, Ashby MR. Cellular solids: structure and properties. Oxford: Pergamon Press; 1988.
[24] Roberts AP, Garboczi EJ. Elastic moduli of model random three-dimensional closed-cell cellular solids. Acta Mater 2001;49:189–97.
[25] Ishai O, Choen LJ. Elastic properties of filled and porous composites. Int J Mech Sci 1967;9:539–46.
[26] Narkis M. Some mechanical properties of particulate-filled thermosetting and thermoplastic polymers. J Appl Polym Sci 1976;20(6):1597–606.
[27] Fredel MC, Boccaccini AR. Processing and mechanical properties of biocompatible Al_2O_3 platelet reinforced TiO_2. J Mater Sci 1996;31:4375–80.
[28] Rezwan K, Chen QZ, Blaker JJ, Boccaccini AR. Biodegradable and bioactive porous polymer/inorganic composite scaffolds for bone tissue engineering. Biomaterials 2006;27:3413–31.
[29] Barry JJA, Nazhat SN, Rose FRAJ, Hainsworth AH, Scotchford CA, Howdle SM. Supercritical carbon dioxide foaming of elastomer/heterocyclic methacrylate blends as scaffolds for soft tissue engineering. J Mater Chem 2005;15:4881–8.
[30] Nazhat SN, Joseph R, Wang M, Smith R, Tanner KE, Bonfield W. Dynamic mechanical characterisation of hydroxyapatite particulate reinforced polyethylene: effect of particle size. J Mater Sci: Mater Med 2000;11:621–8.
[31] Nazhat SN, Kellomäki M, Tanner KE, Tormälä P, Bonfield W. Dynamic mechanical characterisation of biodegradable composites of hydroxyapatite and polylactides. J Biomed Mater Res (Appl Biomater) 2001;58:335–43.
[32] Boccaccini AR, Blaker JJ, Maquet M, Chung W, Jérôme R, Nazhat SN. Poly(D,L-lactide) (PDLLA) foams with TiO_2 nanoparticles and PDLLA/TiO_2-Bioglass® foam composites for tissue engineering scaffolds. J Mater Sci., available on line 7 June 2006.